

Bahaa T. Chiad<sup>(1)</sup>  
 Zainab S. Sadiq<sup>(1)</sup>  
 Dunia K. Mahdi<sup>(1)</sup>  
 Fatin H. Mohammed<sup>(2)</sup>

<sup>(1)</sup> Department of Physics,  
 College of Science,  
 University of Baghdad,  
 Baghdad, Iraq

<sup>(2)</sup> Department of Physics,  
 College of Science,  
 Almustansiriyah University,  
 Baghdad, Iraq

# Structural Characteristics of $\gamma$ - $\text{Al}_2\text{O}_3$ Nanoparticles Prepared by Laser-Assisted Spray Pyrolysis Technique

*This work describes laser-assisted spray pyrolysis (LASP) technique developed to deposit nanoparticles coatings with controllable particles size. In this process, droplets of a precursor formed by atomizer are injected into a deposition chamber using  $\text{SF}_6$  as a carrier gas. The study were focused once on the effect of variation of the concentration of precursor solution on particle size of  $\text{Al}_2\text{O}_3$  samples, and the other effect of variation of  $\text{SF}_6$  gas flow rate on the particle size of the samples. Decreasing of precursor concentration (0.25-0.1M) caused to decrease of the particle sizes with increase in density of  $\text{Al}_2\text{O}_3$  nanoparticles. Decreasing of  $\text{SF}_6$  gas flow rate (4.5-2.5) L/min caused to decrease of the particle sizes with increase in density of  $\text{Al}_2\text{O}_3$  nanoparticles and homogeneity of the samples.*

**Keywords:** Alumina; Nanoparticles; Laser-assisted spray pyrolysis; Coatings

## 1. Introduction

Aluminum oxide ( $\text{Al}_2\text{O}_3$ ) is currently one of the most useful oxide ceramics, as it has been used in many fields of engineering such as coatings, heat resistant materials, abrasive grains, cutting materials and advanced ceramics. This is because alumina is hard, highly resistant towards bases and acids, allows very high temperature applications and has excellent wear resistance [1]. As well, aluminum oxide thin films have several important applications in technology for example in optoelectronics, tribology, sensorics, nanolithography because of their attractive properties. These films have been prepared by various techniques as magnetron sputtering [2], atomic layer deposition [3,4,5], electron beam evaporation [6,7]

Alumina exists in a variety of meta-stable structures including  $\gamma$ -,  $\eta$ -,  $\delta$ -,  $\theta$ -,  $\kappa$ - and  $\chi$ - aluminas [8]. Among various structures for alumina,  $\gamma$ -alumina is one kind of extremely important nanosized materials. It is used as a catalyst and catalyst substrate in automotive and petroleum industries, structural composites for spacecraft, and abrasive and thermal wear coatings [9]. Recent studies have shown that  $\gamma$ -alumina is thermo dynamically stable relative to  $\alpha$ -alumina when a critical surface area is achieved [10].

## 2. Experiment

Laser-assisted spray pyrolysis (LASP) technique set-up consists mainly of the ultrasonic nebulizer, deposition chamber, temperature control, and CW  $\text{CO}_2$  laser. Generally, the nebulizer is operated at a frequency of 1.7 MHz, where the precursor solution is converted into a mist of particles in the range of 1-5  $\mu\text{m}$  in diameter. The diameter of the particle has a dependency on the operating frequency of the nebulizer according to the Lang's equation [11]:

$$d = 0.34 \left( \frac{8\pi\gamma}{\rho \cdot f^2} \right)^{\frac{1}{3}} \quad (1)$$

where  $\gamma$  is the surface tension,  $\rho$  is the density of the atomized solution and  $f$  is the frequency of the ultrasound waves

However the deposition process was carried out inside of deposition chamber, it made from stainless steel.

In LASP technique set-up, the solution was sprayed downward as shown in Fig. (1). An aqueous ethanol ( $\text{H}_2\text{O}:\text{Et}=1:1$ , in volume ratio) solutions of  $\text{AlCl}_3 \cdot 6\text{H}_2\text{O}$  (molecular weight = 133.34g/mol) (98.5% pure, Fluka-Garantin) were used as precursors for the alumina films with different concentrations.

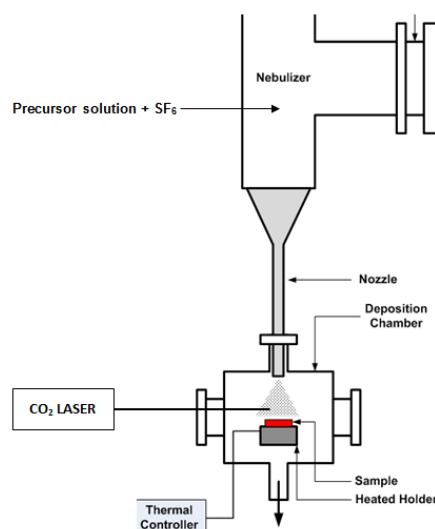


Fig. (1) Schematic diagram of the LASP experimental setup

The glass substrates were cleaned with an ultrasonic agitator in repeated baths of ethanol and acetone, and then rinsed in distilled water prior to loading into the chamber. Next, prepared substrate was set up on the substrate holder 10 cm away from the nozzle and the holder was heated to 450 °C. The nebulizer filled with precursor solution, the chamber was continually pumped by a vacuum pump to maintain the ambient pressure about 760 mmHg. The process was run for 20min to get a good layer of Al<sub>2</sub>O<sub>3</sub>. Several samples were synthesized, once, by changing the concentration (0.1, 0.15, 0.2 and 0.25) M. CW CO<sub>2</sub> laser of 3W was focused to a point just above the funnel tube orifice, while sulfur hexafluoride (SF<sub>6</sub>) which used as a carrier gas for aerosol transport at 3.5 L/min flow rates and other with different of SF<sub>6</sub> gas flow rate (2.5, 3.5, 4.5) L/min.

X-ray diffraction (XRD) studies were carried out on a Bruker AXS D2 PHASER diffractometer, working with the K $\alpha$  line of copper ( $k=0.154\text{nm}$ ). Measurements of the samples were carried out in the range  $2\theta$  of 20-60°, infrared spectra were recorded with Shimadzu FTIR-8400 spectrophotometer in the range from 4000 to 400 cm<sup>-1</sup>. SEM characterization of gamma alumina was carried out with scanning electron microscopy (model Hitachi 4160).

### 3. Result and Discussion

Figure (2) shows the x-ray diffraction (XRD) pattern, in which the peaks belonging to the crystalline phases of Al<sub>2</sub>O<sub>3</sub> (311), (222), and (400) are observed. All of the observed peaks can be assigned to the  $\gamma$ -Al<sub>2</sub>O<sub>3</sub> phase in accordance with data from the ASTM (American Society of Testing Materials) cards as well as the average crystallite size were calculated using the Scherrer's equation. Table (1) illustrates the grain size of the prepared samples.

Figure (3) shows the Fourier-transform infrared (FTIR) spectra of alumina (Al<sub>2</sub>O<sub>3</sub>) samples prepared by LASP technique. As can be observed, the stronger broadening band at 3800-3000 cm<sup>-1</sup> is attributed to the hydrogen bond between the various hydroxyl groups in the product. As well, the stronger broadening band at 1000-400 cm<sup>-1</sup> corresponds to Al-O vibration. Our results are agreed with Hosseini et al [12].

The surface morphology of alumina samples prepared by LASP technique with using various

precursor concentrations (0.1, 0.15, 0.2, 0.25) M are presented in Fig. (4). Table (2) illustrates the effect the concentration of precursor solution on the size and shape of Al<sub>2</sub>O<sub>3</sub> nanoparticles which was prepared by LASP technique.

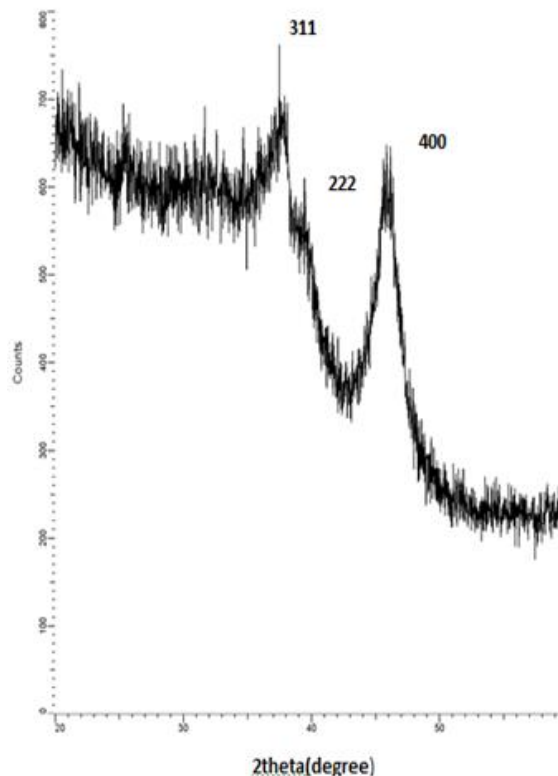


Fig. (2) X-ray diffraction (XRD) pattern of a  $\gamma$ -Al<sub>2</sub>O<sub>3</sub> nano-grained sample prepared by LASP

Table (2) Effect of precursor concentrations on size and shape of Al<sub>2</sub>O<sub>3</sub> particles which prepared by LASP technique

Concentration of precursor solution (M)	The size range of particle LASP (nm)	Shape of particle by LASP
0.1	17-49	Spherical
0.15	23-55	Cubic
0.2	28-57.8	Cubic + Oblang
0.25	31-66	Cubic + agglomerated cubic

Table (1) Experimental and standard values of peaks, and grain size for prepared  $\gamma$ -Al<sub>2</sub>O<sub>3</sub> sample by LASP technique

$2\theta$ (deg)	$d_{hkl}$ (Exp.) (Å)	$d_{hkl}$ (Std.) (Å)	hkl	FWHM (deg)	G.S (nm)	Phase
37	2.429	2.39	311	0.8	12.55	$\gamma$ -Al <sub>2</sub> O <sub>3</sub>
39.1	2.3	2.28	222	0.3	42.04	$\gamma$ -Al <sub>2</sub> O <sub>3</sub>
45.9	1.98	1.977	400	1.2	25.05	$\gamma$ -Al <sub>2</sub> O <sub>3</sub>

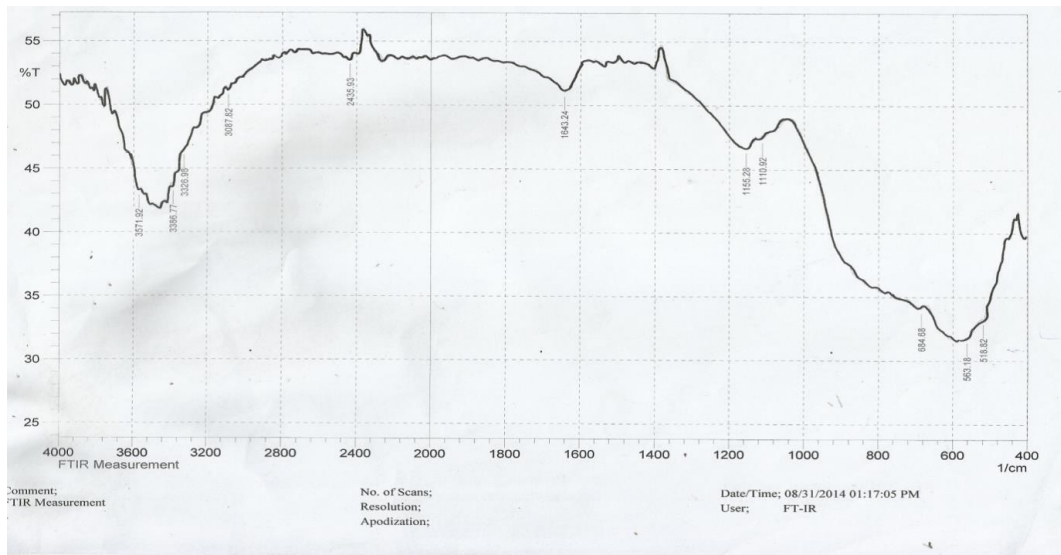
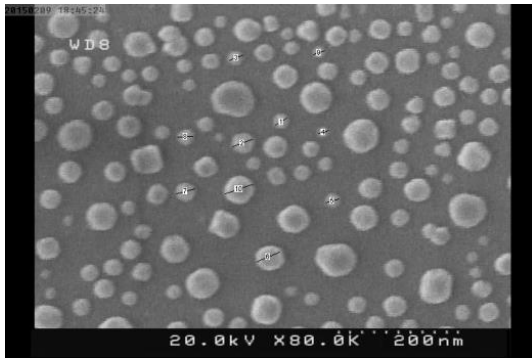
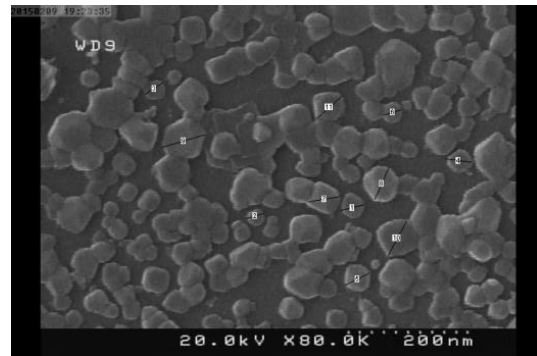


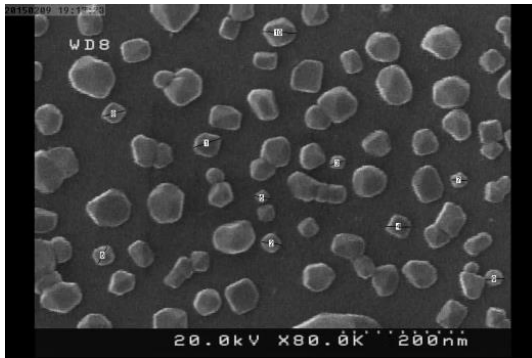
Fig. (3) FTIR spectra of  $\gamma$ -Al<sub>2</sub>O<sub>3</sub> sample which prepared by LASP



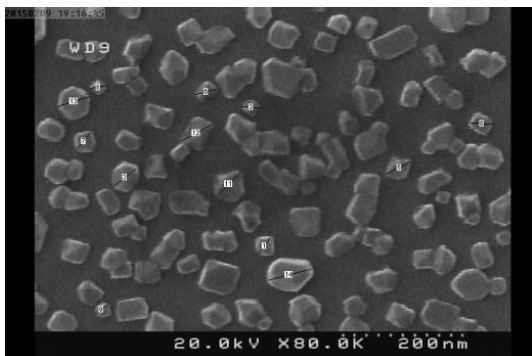
(a)



(d)



(b)



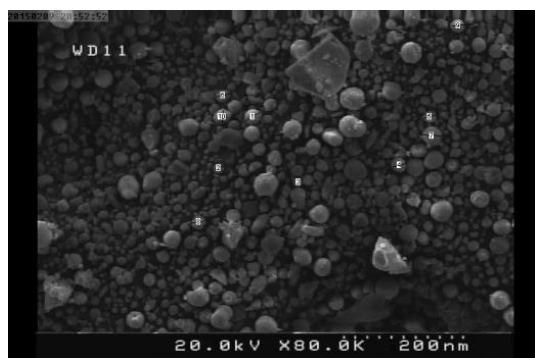
(c)

Fig. (4) SEM images of Al<sub>2</sub>O<sub>3</sub> samples obtained at different precursor concentrations (a) 0.1, (b) 0.15, (c) 0.2, and (d) 0.25 M

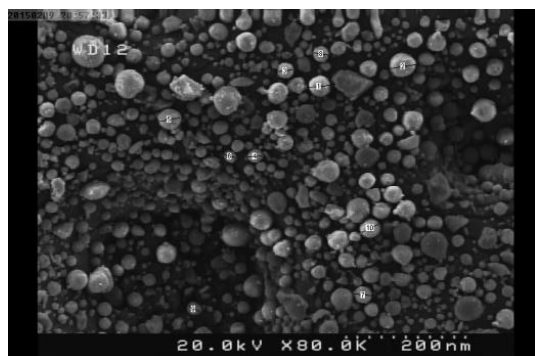
Figure (5) shows the SEM images and table (3) of  $\gamma$ -Al<sub>2</sub>O<sub>3</sub> nanoparticles synthesized at different SF<sub>6</sub> gas flow rate (2.5, 3.4, 4.5) L/min respectively with substrate temperature 450°C and 0.15M (where 0.15 is the perfect concentration to get a good layer with constant of the others parameters).

Table (3) Effect of SF<sub>6</sub> gas flow rate on size and shape of Al<sub>2</sub>O<sub>3</sub> particles which prepared by LASP technique

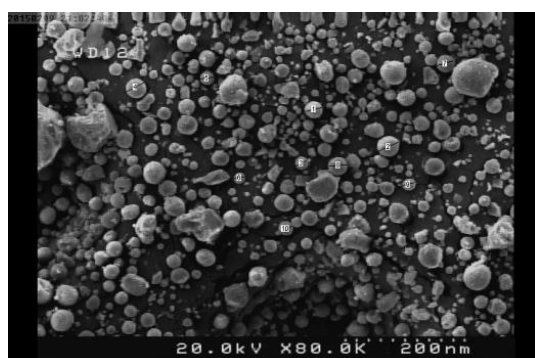
SF <sub>6</sub> gas flow rate L/min	Particle size (nm)	Shape of particle
2.5	9-26	Spherical
3.5	12-35	Spherical
4.5	16-36	Spherical



(a)



(b)



(c)

**Fig. (5)** SEM micrograph of  $\text{Al}_2\text{O}_3$  samples obtained at different flow rate of  $\text{SF}_6$  gas (a) 2.5, (b) 3.5, and (c) 4.5 L/min

From experimental results it can be concluded that the decrease of  $\text{SF}_6$  flow rate has a positive influence on particle size distribution where the particle size

decreases with a decrease in the flow rate of the carrier gas. This is due to the fact that when the flow rate decreases, the droplet spends more time in contact with the laser, thus absorbing more energy and resulting in smaller particles.

#### 4. Conclusions

Gamma-phase ( $\gamma$ ) alumina nanoparticles were successfully synthesized using the LASP technique. The experiments show that by controlling the precursor concentration, a further reduction in particle size is observed, and with a decrease in  $\text{SF}_6$  gas flow rate, the particle size also decreases.

#### Acknowledgment

The authors would like to thank Dr. Oday Hammadi at Al-Iraqia University in Baghdad for his assistance in the preparation and publication of this article.

#### References

- [1] A.A.I.Y. Tok, F.Y.C. Boey and X. L. Zhao, *J. Mater. Process. Technol.*, 178, 270–273, 2006.
- [2] J. Houska et al., *Thin Solid Films*, 520, 5405–5408 (2012).
- [3] M.D. Groner et al., *Thin Solid Films*, 413, 186–197 (200).
- [4] Y. Kim et al., *Appl. Phys. Lett.*, 71, 3604–3606 (1997).
- [5] P. Kumar et al., *Appl. Opt.*, 48, 5407–5412 (200).
- [6] N. Maiti et al., *Vacuum*, 85, 214–220 (2010).
- [7] P.V. Patil et al., *Thin Solid Films*, 288, 120–124 (1966).
- [8] S. Wang et al., *Mater. Lett.*, 62, 3552–3554, 2008.
- [9] G. Paglia et al., *Chem. of Mater.*, 16, 220, 2004.
- [10] Y.H. Wang et al., *J. Alloys Compounds*, 467, 405–412, 2009.
- [11] S. Stopic et al., *J. Metallurgy*, UDC:669-492:621.762.2.084.8(n)=20 42-54.
- [12] S.A. Hosseini, A. Niaei and D. Salari, *Open J. Phys. Chem.*, 1, 23–27, 2011.